Close interactions of 3D vortex tubes

By M. V. MELANDER[1]

Abstract

The motivation for studying close vortex interactions is briefly discussed in the light of turbulence and coherent structures. Particular attention is given to the interaction known as reconnection. Two reconnection mechanisms are discussed. One is annihilation of vorticity by cross-diffusion, the other is an inviscid head-tail formation. At intermediate Reynolds numbers both mechanisms are operating.

1. Introduction

Close interaction and self-deformation of vortices are intriguing facets of fluid mechanics. These interactions occur repeatedly in turbulent flows. We can, therefore, expect that insight into fundamental vortex interactions will lead to a deeper understanding of turbulence. The theory of turbulence in 2D flows illustrates this point clearly. In 2D flows fundamental vortex interactions such as axisymmetrization, merger, and dipole formation provide the mechanisms for the emergence of large scale coherent structures (McWilliams 1984). These structures in turn invalidate earlier statistical theories based on random phases (Babiano et al 1987). Compared to 2D vortex dynamics, our understanding of three dimensional vortex interactions is in its infancy. In order to improve this level of understanding, it seems logical to begin by investigating the most basic vortex interactions. This report marks the beginning of a thorough investigation of such interactions.

We confine the study to unforced incompressible flows with no density variations and unbounded domains. Turbulence may then be viewed as a tangle of interacting vortices. This follows directly from the integral formulation of Navier-Stokes equations.

$$\mathbf{u}(\mathbf{r}) = \frac{1}{4\pi}\int \frac{\boldsymbol{\omega}(\mathbf{r}')\times(\mathbf{r}-\mathbf{r}')}{|\mathbf{r}-\mathbf{r}'|^3}d\mathbf{r}' + \nabla\phi \tag{1}$$

$$\boldsymbol{\omega} = \nabla\times\mathbf{u} \tag{2}$$

$$\frac{D\boldsymbol{\omega}}{Dt} = (\boldsymbol{\omega}\cdot\nabla)\mathbf{u} + \nu\Delta\boldsymbol{\omega} \tag{3}$$

1 Permanent address: SMU, Texas

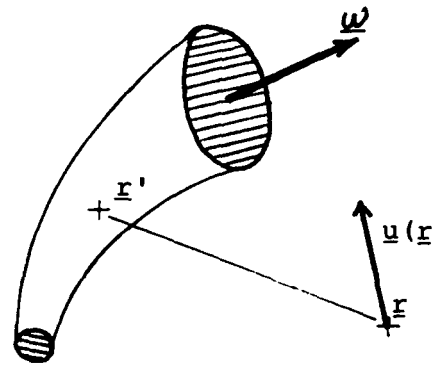

FIGURE 1. Schematic for the calculation of the velocity field $u(\mathbf{r})$ generated by a vortical structure.

When the fluid is at rest at infinity, the potential component in (1) vanishes. The Biot-Savart law (1) then shows that the vorticity governs the flow. The vorticity transport equation (3) in turn describes how the vorticity evolves with the flow. Some attractive features of the formulation (1) - (3) are: I) The irrotational part of the fluid does not appear in this description. This fact is the motivation behind computational methods known as "vortex methods" (Leonard 1985). Unfortunately, these methods make strong assumptions concerning the local vorticity distribution and may need further development before they can safely be used to investigate delicate vortex interactions. II) The description (1) - (3) appeals to our physical intuition. It is conceptually easy to give a qualitative prediction of the short time evolution of a given vorticity configuration by means of arm-waving and finger-twisting arguments. It is also possible to understand vortex dynamics in terms of primitive variables and force-balancing (Moore and Saffman 1972); although this approach leads to the same physical results, it seems considerably more complicated. III) A systematic description of how the small scale vortical structures influence the far-field $u(r)$ can be obtained from the Biot-Savart law (1).

Let us consider the last point in detail. Let a vorticity configuration be given near position $\mathbf{r}'$ (Figure 1). The Biot-Savart integral gives the velocity field $\mathbf{u}(\mathbf{r})$ generated by this vorticity configuration at position $\mathbf{r}$. The integration extends over the entire vorticity configuration. Clearly the integrand depends on $\mathbf{r}$, so it is an enormous task to evaluate the integral for many different $\mathbf{r}$ positions. However, if $|\mathbf{r}' - \mathbf{r}|$ is large, we can expand the integrand in inverse powers of $|\mathbf{r}' - \mathbf{r}|$. The coefficients in this expansion are moments of the vorticity configuration and hence independent of $\mathbf{r}$. These moments describe the shape and internal structure of the vorticity configuration. Far away, only the lowest order moment matters, but as we let $\mathbf{r}$ approach the vorticity configuration, an increasing number of moments must be included. We see that physical space moments yield a systematic description of internal structures influence on the

far-field. This idea has been used with success in 2D (Melander et al 1986).

The above discussion shows that the interaction between well separated vortices can be calculated efficiently in a straightforward manner. However, when $|\mathbf{r} - \mathbf{r}'|$ is small, we are faced with an entirely different situation. We no longer have a natural expansion parameter for the evaluation of the Biot-Savart integral. The integrable singularity in (1) tends to amplify the influence of the local structure. As a consequence, the local self-induced velocity can become very large for slender vortices. Such slender vortices can easily develop through vorticity stretching. A more subtle effect of small scale vorticity lies in its ability to alter neighboring large scale vortical structures. A concrete example from 2D is the axisymmetrization of a single isolated vortex (Melander et al 1987); here the small scale structures (filaments) influence the large scales in such a way as to make the vortex core circular symmetric. Because of these effects, we must treat the local vorticity structure and the associated small scales carefully. A thorough study of close vortex interactions via direct numerical simulations will, therefore, be most helpful for modelling of the local vorticity distributions and the associated small scales.

Vortex dynamics reveals its most useful role when viewed in the light of coherent structures. These vortical structures have been observed in many flows that were previously regarded as fully random (Hussain 1986). Often these large scale structures are superimposed by fluctuating vorticity (incoherent vorticity), which makes the structures less obvious, but not less important. In spite of the incoherent vorticity, the large structures still dominate the far-field. The incoherent vorticity does not influence the far-field directly, but can have an indirect influence by altering neighboring structures, as discussed above. Many interesting questions arise concerning the formation, persistence, characterization, topology, and interaction of coherent structures. Some of these questions are best approached through vortex dynamics. In this report we concentrate on interactions that can change the topology. These interactions are generally known as reconnections, although other names such as cut-and-connect, cross-linking, and fusion are also used. We examine a number of reconnection interactions under very idealized conditions. The interactions are simulated in isolation such that non-local effects do not obscure the dynamics. Also, there is no incoherent vorticity in our initial conditions.

2. Initial Conditions, Simulation Methods, and Diagnostics

The simulations were performed using a dealiased spectral (Galerkin) method with a fourth order predictor-corrector algorithm for the time advancement. This algorithm solves the Navier-Stokes equations (or the corresponding equations with superviscosity) in a cube with periodic boundary conditions. The evolution of a passive scalar at a unity Schmidt number is calculated simultaneously. The initial conditions (Figure 2a-f) were chosen as rectilinear vortices with a Gaussian vorticity profile. The evolution starting from the initial condition

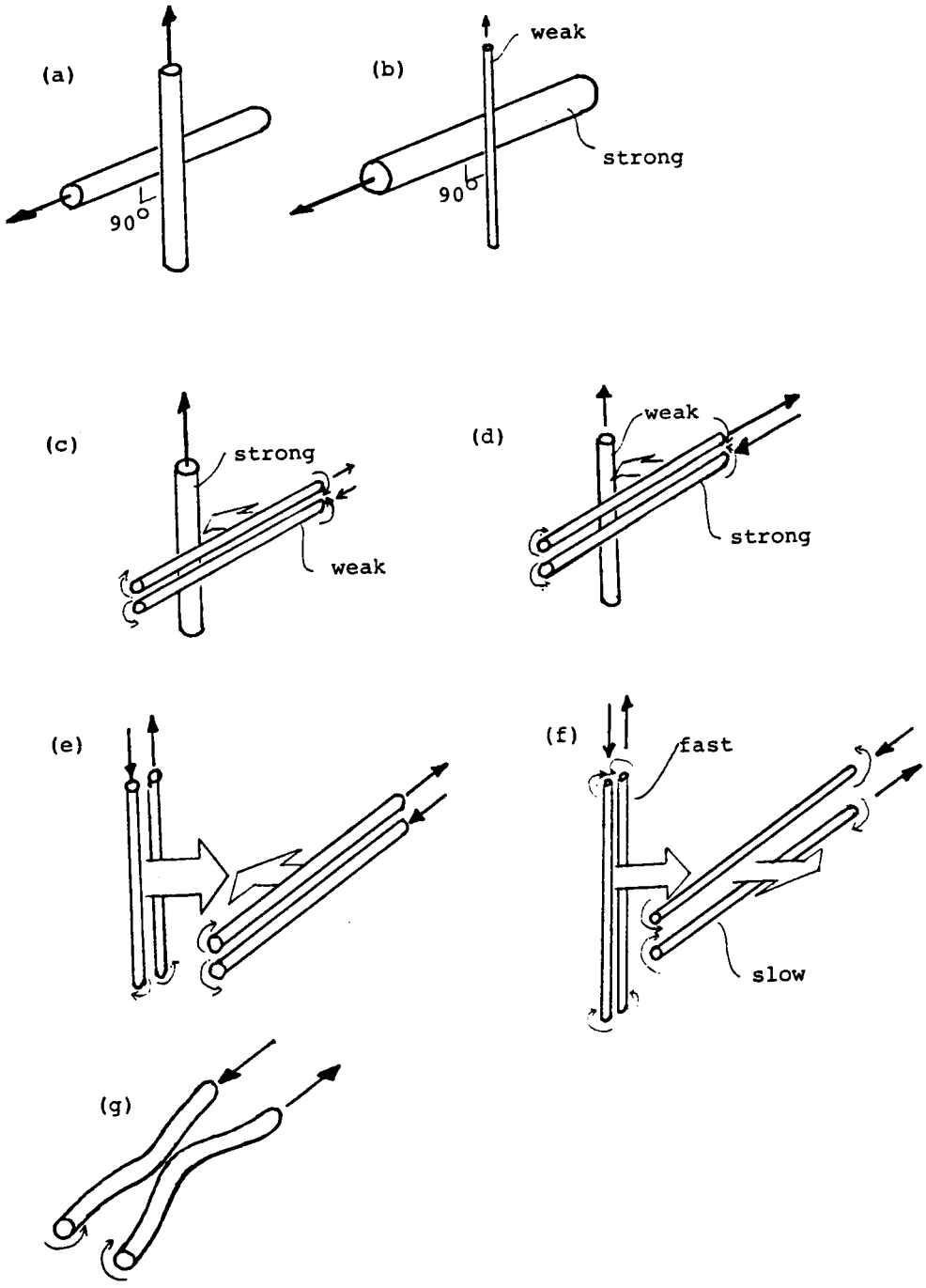

FIGURE 2. Initial conditions for the simulations.

shown in Figure 2a was simulated using both Newtonian viscosity ($Re = 2000$) and superviscosity, while in the cases (b-f) only superviscosity was used. The spatial resolution in all these cases was 96 meshpoints in each direction. The simulation starting from the initial condition shown in Figure 2g is discussed at great length elsewhere (Melander and Hussain 1988 a,b,c).

The simulations produced databases which were analyzed on graphics workstations using the "interactive" program TURB3D. Displays of the spatial vorticity distribution at various stages of the evolution were crucial in obtaining a physical understanding of the interactions. Cross sections of vorticity and velocity fields were also very helpful, whereas displays of other quantities such as helicity, dissipation, and enstrophy production were found to be of secondary importance. Tracing of vortex-lines turned out to be a major disappointment, for it seemed impossible to find just the right set of vortex lines to clearly illustrate a given interaction. In general, a few vortex-lines were not enough to reveal the dynamics, while a larger number such as 20 gave a picture that was too complicated to follow. Perhaps displays of vortex tubes via Clebsch potentials would be more appropriate.

3. Discussion

In order to achieve a higher effective Reynolds number, a superviscosity was used in most simulations. The superviscosity leaves the largest scales more inviscid than does a corresponding Newtonian viscosity. However, it is also known that the superviscosity generates artificial small scale structures. Comparison of two simulations, starting from the same initial condition (Figure 2a) but with different diffusion operators, showed similar evolutions. The most important difference between these two simulations was the evolution time-scale; it was shorter in the superviscosity simulation. A similar effect has also been observed by decreasing the Newtonian viscosity, and hence increasing Reynolds number. We therefore conclude that the use of a superviscosity mimics a higher Reynolds number flow and that the artificial small scale structures do not significantly influence the large scale structures.

Inviscid filament calculations with regularized circular cores show that two orthogonally offset vortices become locally antiparallel (Schwarz 1983 and 1985, Siggia 1985). Careful studies show that if the same filament calculations are continued further in time, then a finite-time singularity develops (Pumir and Siggia 1987). This singularity is most likely caused by insufficient degrees of freedom in the vortex cores, that is, inadequate modelling. Nevertheless, some researchers feel that a similar singularity might be present in the full Euler equations (Pumir and Kerr 1987, Kerr and Hussain 1988). It has also been suggested that this singularity is present in the Navier-Stokes equations at sufficiently high Reynolds number (Pumir and Siggia 1987). Direct numerical simulations have failed to capture signs of this singularity.

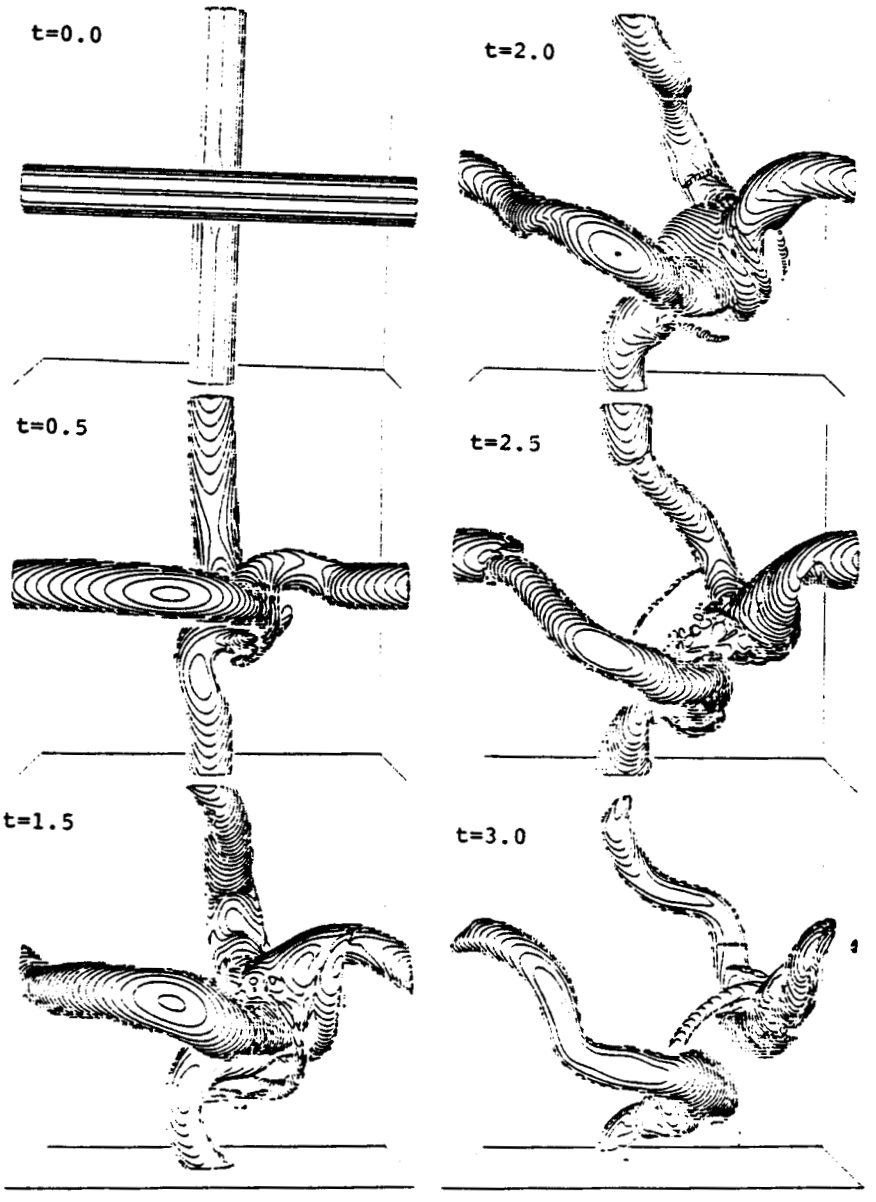

FIGURE 3. Evolution of the initial condition shown in Figure 2a at Reynolds number 2000. The panels show isovorticity surfaces at 56% of the initial peak value. Time is measured in units of $\omega_{\max}(0)/20$.

Since it is almost impossible to prove or disprove the presence of a singularity numerically, a more fruitful avenue is to concentrate on understanding the operating physical mechanisms. One can argue that if it is possible to explain the evolution without including new terms in the governing equations, then there probably is no singularity. This argument rests on the general experience that a singularity is a sign of missing physics in the governing equations.

The evolution starting from the initial condition shown in Figure 2a highlights the soft and pliable nature of vortex cores, thereby clearly showing that vortex cores do not remain nearly circular. The close proximity of the vortices results in pulling of hairpins from the outer layer of the vortex tubes (Figure 3). These hairpins form even before the main vortex tubes become locally antiparallel. Later more hairpins form, especially in the wake of the locally antiparallel vortex pair (hereafter referred to as the dipole).

The dipole is initially squashed by self-induction (due to the curvature of the antiparallel vortex pair) and thereby form a head-tail structure. The dipole is propagating by mutual induction. However, an oppositely directed velocity field is generated by the remaining part of the vortex tubes. At first the dipole velocity is the largest, but later the dipole-strength diminishes and as a result the dipole is washed backwards. Thereby the curvature of the locally antiparallel vortices reverses, the self-induced motion, therefore, also reverses, and the dipole separates slowly. This reversal is the crucial part of the reconnection process and occurs at the same time as the new "reconnected" vortices begin to separate (Figure 3).

The reversal is caused by the diminishing dipole-strength, which can happen by both a diffusive and an inviscid mechanism. The diffusive mechanism is annihilation of antiparallel vorticity by cross-diffusion in the contact-zone and is clearly important for low to medium Reynolds numbers. The result is a true reconnection, albeit this reconnection is only partial as the cross-diffusion is arrested by the reversal of the dipole propagation direction (Melander and Hussain 1988a). The inviscid mechanism is the head-tail formation. The dipole propagation velocity is determined almost exclusively by the head; therefore, the head-tail formation effectively diminishes the circulation in the dipole. In the high Reynolds number limit, this may result in an apparent reconnection. That is, the large scale vortical structures appear as though a topological reconnection has occurred, where in fact only a topology preserving entanglement has taken place. The reasons for this conjecture are as follows.

Several numerical simulations with different Reynolds numbers and different diffusion operators show that the large scale vortical structures rearrange on a time-scale T, which does not increase with Reynolds number. Weakening of the dipole is responsible for this rearrangement. If viscous effects are solely responsible for this weakening, then $|\nu\Delta\omega|$ must be at least finite as the Reynolds number tends to infinity. This in turn implies that $|\Delta\omega|$ must become unbounded within the finite time T, which can only happen through axial stretching of the

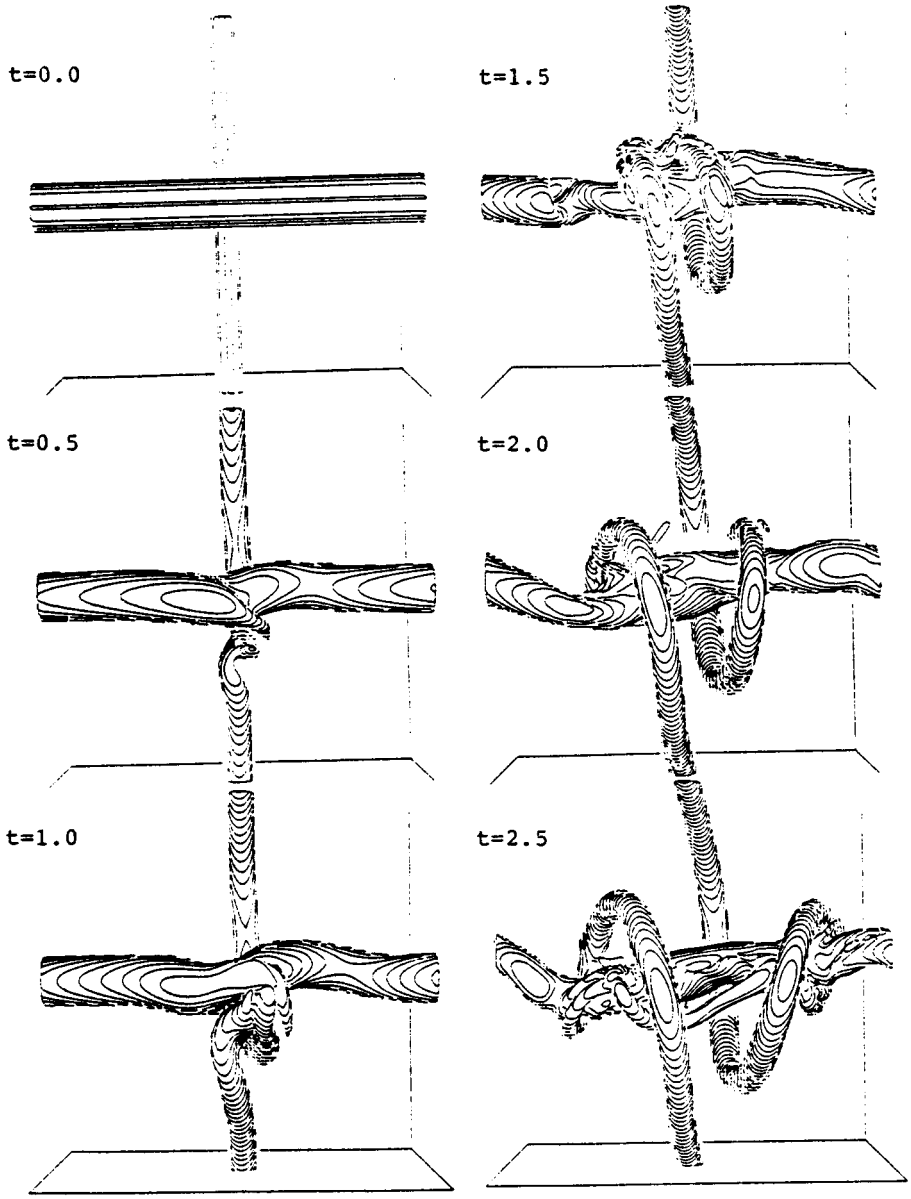

FIGURE 4. Asymmetric entanglement and apparent reconnections; the circulation ratio is four. The isosurface level and timescaling are the same as in Figure 3.

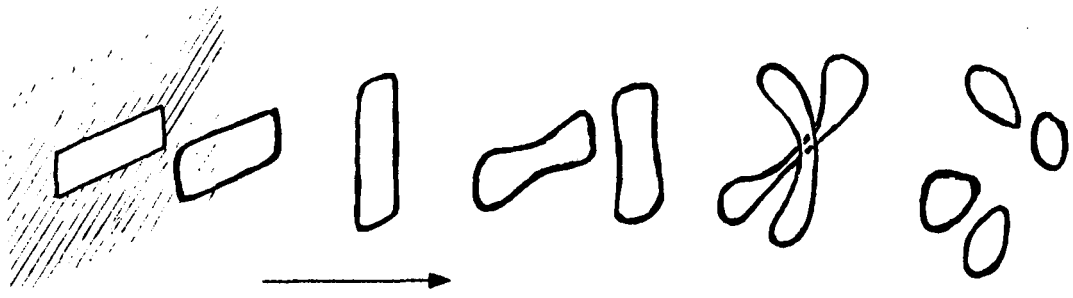

FIGURE 5. Sketch of Husain and Hussain's rectangular jet experiment.

dipole. This stretching is caused by lengthening of the antiparallel vortices in the contact-zone and by the strain form outside the contact-zone. From axisymmetric vortex dynamics (Stanaway et al 1988), we know that the lengthening effect is insufficient to cause a finite time blow up of $|\Delta\omega|$. The external strain is also bounded due to the finite length of the contact-zone.

Neither of the simulations starting from the initial condition shown in Figure 2a had sufficient resolution to clearly separate the inviscid and viscous mechanisms. It does not seem likely that sufficient resolution can be obtained in the near future. In this respect the asymmetric initial condition (Figure 2b) is more promising due to the fact that the circulation ratio can be made small such as to allow for combined simulation and analysis. The dynamics of this simulation is also much easier to grasp, see Figure 4. The weak vortex wraps around the stronger one and thereby forms a large hairpin. Vortex stretching occurs mainly in the legs of the hairpin. The tip of the hairpin is unstretched and dispersed in the azimuthal direction. Therefore, the curvature of the legs accounts for most of the self-induced motion, which is such as to split the hairpin into two diverging helical structures.

The evolutions of the initial conditions shown in Figures 2c-f were also investigated and explained. I later became aware that the latter occurs in a rectangular jet experiment by F. Hussain, see Figure 5. Pulsing of the jet generates rectangular vortex rings, which initially undergo a near-recurrence with 90 ° axis-flip. This phenomenon can be explained by a filament model (Bridges and Hussain 1988), except for rapid mixing processes near the corners. Further downstream an overtaking collision occurs and the resulting reconnections produce four rings. The overtaking collision occurs because the rectangular vortex

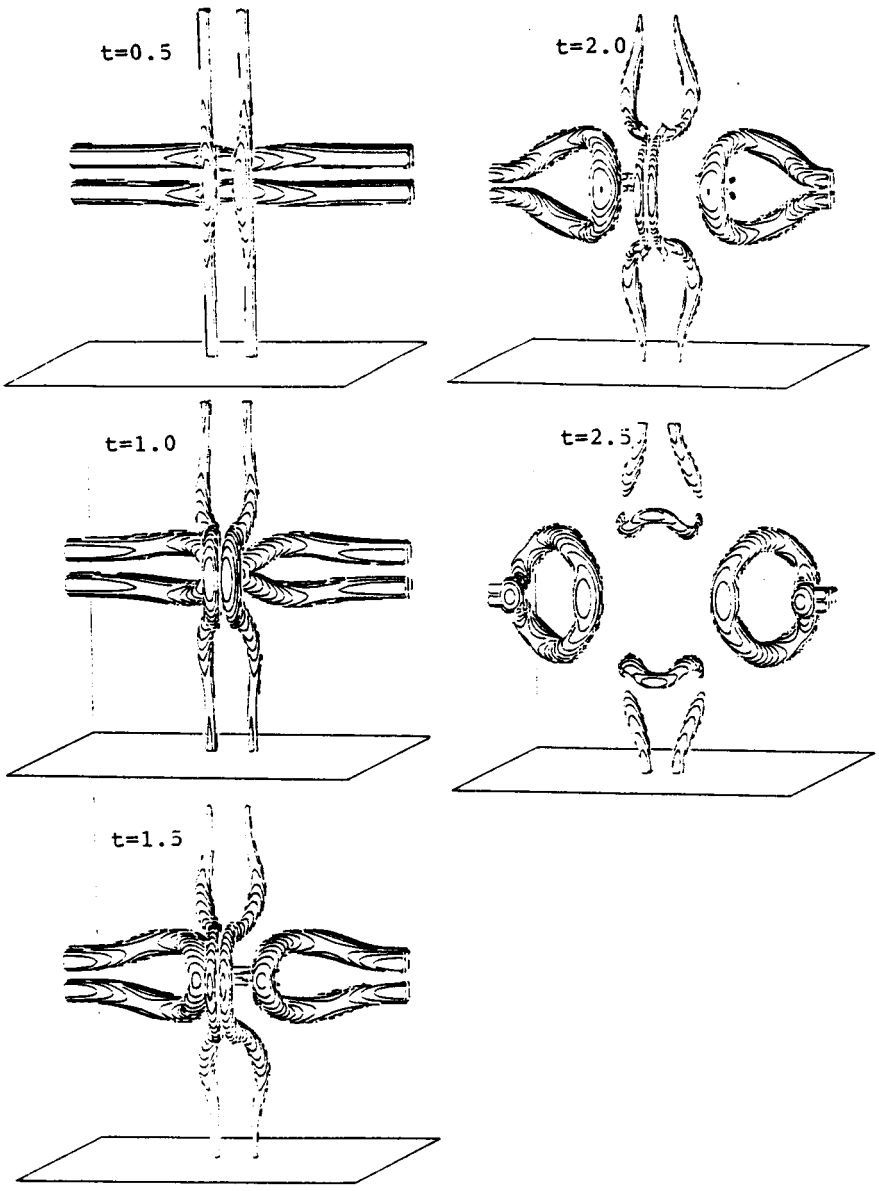

FIGURE 6. Simulation of an overtaking collision; the fast vortex pair has twice as much circulation as the slow pair. The isosurface level and timescaling are the same as in Figure 3.

rings do not comply with the traditional leap-frog process of axisymmetric vortex rings. The experiment compares well with the simulation shown in Figure 6 and clearly validates our selection of idealized initial conditions.

4. Conclusion

The insight gained by viewing the evolutions of the above idealized initial conditions on graphics workstations has proved to be invaluable in the process of constructing mathematical models of the evolutions. The modelling, which is now under way, centers around two types of initial conditions. One type is the symmetric configuration of two antiparallel vortices with sinusoidal perturbations (Figure 2g). The analysis of this model also applies to the collisions shown in Figure 2e-f. The asymmetric entanglement shown in Figure 2b and Figure 4 is also being modelled for small values of the circulation ratio.

Acknowledgement

The simulations were done at Pittsburgh Supercomputing Center and were diagnosed on workstations at NASA-Ames. I gratefully acknowledge Dr. K. Shariff for help with the workstations and many helpful discussions. Furthermore, I acknowledge Prof. F. Hussain for pointing out the connection with coherent structures.

REFERENCES

BABIANO, A., BASDEVANT, G., LEGRAS, & B., SADOURNY, R. 1987 *J. Fluid Mech.* **183,** 379-398.

BRIDGES, J. & HUSSAIN, F. 1988 *Bull. Amer. Phys. Soc.* **33,** 2306.

HUSSAIN, FAZLE, A. K. M. 1986 *J. Fluid Mech.* **173,** 303-356

KERR, R. M. & HUSSAIN, F. 1988 *Physica D.* (Subjudice).

LEONARD, A. 1985 *Ann. Rev. Fluid Mech.* **17,** 523-59.

MCWILLIAMS, J. C. 1984 *J. Fluid Mech.* **146,** 21-43.

MELANDER, M. V., ZABUSKY, N. J., & STYCZEK, A. S. 1986 *J. Fluid Mech.* **167,** 95-115.

MELANDER, M. V., & HUSSAIN, F. 1988 Center for Turbulence Research. Proceedings of the summer program 1988. (to appear)

MELANDER, M. V., & HUSSAIN, F. 1988 *Phys. Rev. Lett.* (Subjudice).

MELANDER, M. V., & HUSSAIN, F. 1988 *Phys. of Fluids* (Subjudice).

MOORE, D. W., & SAFFMAN, P. G. 1972 *Philos. Trans. R. Soc. London Ser. A* **272,** 403-429.

PUMIR, A. & KERR, R. 1987 *Phys. Rev. Lett.* **58,** 1636.

SCHWARZ, K. W. 1983 *Phys. Rev. Lett.* **50,** 364.

SCHWARZ, K. W. 1985 *Phys. Rev. B* **31**, 5782.

SIGGIA, E. D. 1985 *Phys. of Fluids* **28**, 794.

STANAWAY, S., SHARIFF K., & HUSSAIN, F. 1988 CTR Proceedings of the 1988 Summer Program, 287-309.